Solving the Fully Coupled Time-Dependent Maxwell-Dirac System: A Second-Order Accurate Numerical Scheme

Jul Van den Broeck, Emile Vanderstraeten, Pieter Decleer, Dries Vande Ginste

quest, IDLab, Department of Information Technology, Ghent University
Technologiepark-Zwijnaarde 126, B-9052 Gent, Belgium

***Abstract*—Owing to their increased carrier velocities, Dirac materials have become a promising option for the integration into nanoelectronics. However, without the aid of simulation software that is able to accurately describe the behavior of these materials, the fabrication of novel devices is extremely challenging. In this work, we present a second-order accurate, multiphysics solution method for the pertinent time-dependent Maxwell-Dirac equations. The numerical stencils of the separate equations are presented, leading to a novel stability criterion for the minimally coupled Dirac equation. Afterwards, the second-order accuracy is demonstrated via a numerical example, in which a Dirac particle is represented as a wave packet.**

***Index Terms*—Nanoelectronics, computational electromagnetics, relativistic quantum mechanics, finite-difference time-domain methods, numerical stability**

I. Introduction

Since the last decade, the dimensions of transistors are reaching the physical limit. To tackle the troublesome quantum effects that emerge at this scale, new research paths are being explored. In performance-enhancing Dirac materials, such as graphene, topological insulators, Weyl semimetals, and Dirac semimetals, electrons obey Dirac-like Hamiltonians, allowing for high-mobility carrier transport. The cost-effective design of novel nanoelectronic devices requires modeling tools that incorporate the electromagnetic (EM), quantum mechanical (QM), and relativistic effects appearing in these Dirac materials.

Only a few schemes for the fully coupled (3+1)D Maxwell-Dirac system have been published [1]–[5]. These methods solve the wave equations for the EM potentials, while *implicitly* adopting the Lorenz gauge. The gauge condition is hence not satisfied in general. Furthermore, these methods directly determine the EM potentials $\boldsymbol{a}$ and ϕ, making the integration with well-established EM solvers, which compute the fields $\boldsymbol{e}$ and $\boldsymbol{h}$, very tedious. Moreover, the Dirac spinor in [1]–[5] is discretized on a regular grid, which inevitably leads to the fermion doubling problem [6]. Thus, the development of improved schemes that avoid these inadequacies is still necessary.

We therefore propose a self-consistent solution method for the time-dependent (3+1)D Maxwell-Dirac equations, similar to the work in [7] where the Maxwell-Schrödinger system is dealt with. The Dirac scheme presented in [8] is extended in this paper to describe *charged* Dirac particles, and is coupled with Yee's finite-difference time-domain (FDTD) method for Maxwell's curl equations. This choice makes our solver compatible with existing EM code. Furthermore, the advocated scheme incorporates the discrete Lorenz gauge, which is hence exactly satisfied. Finally, a concrete example of a Dirac wave packet illustrates the overall second-order accuracy of our method.

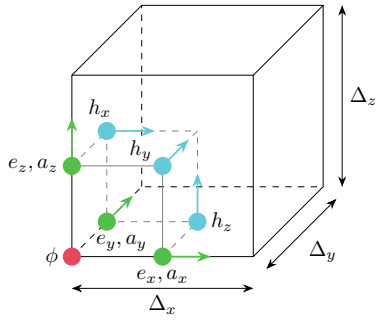

Fig. 1. Schematic depiction of the Yee cell, which contains the spatial grid points on which the discretized EM quantities are defined. The electric quantities $\boldsymbol{e}$ and ϕ are evaluated at half-integer time steps, and the magnetic variables $\boldsymbol{h}$ and $\boldsymbol{a}$ are calculated at integer time steps.

II. Discretization of the Maxwell-Dirac System

A. Maxwell's Equations and the Lorenz Gauge

The EM curl equations for the electric field $\boldsymbol{e}$ and the magnetic field $\boldsymbol{h}$ are discretized according to the FDTD method, yielding

$$\hat{\partial}_t \tilde{\boldsymbol{e}}_{\boldsymbol{m}}^{n+\frac{1}{2}} = \frac{1}{\epsilon_0}\hat{\nabla} \times \hat{\boldsymbol{h}}_{\boldsymbol{m}+\frac{1}{2}}^{n} - \frac{1}{\epsilon_0}\tilde{\boldsymbol{j}}_{\boldsymbol{m}}^{n}, \tag{1a}$$

$$\hat{\partial}_t \hat{\boldsymbol{h}}_{\boldsymbol{m}+\frac{1}{2}}^{n+1} = -\frac{1}{\mu_0}\tilde{\nabla} \times \tilde{\boldsymbol{e}}_{\boldsymbol{m}}^{n+\frac{1}{2}}. \tag{1b}$$

The discrete calculus notation, proposed by W. C. Chew [9], for so-called *fore-* and *back*-vectors is introduced, which are indicated with a tilde and a hat, respectively. Here, μ_0 and ϵ_0 are the vacuum permeability and permittivity, respectively, and $\tilde{\boldsymbol{j}}$ is the discrete current density. The notation $\boldsymbol{m} = (i, j, k)$ and $\boldsymbol{m} + 1/2 = (i + 1/2, j + 1/2, k + 1/2)$ indicates the spatial sites of the discrete vectors, where the integers i, j and k denote the indices of the grid points in each spatial dimension. The index n corresponds to the time step. Fig. 1 displays the position of the fields on a unit cell, referred to as the "Yee cell".

The stability of the FDTD method is guaranteed if the time step Δ_t obeys

$$\mathrm{CN} = c\Delta_t \sqrt{\frac{1}{\Delta_x^2} + \frac{1}{\Delta_y^2} + \frac{1}{\Delta_z^2}} \leq 1, \tag{2}$$

where Δ_l, $l = x, y, z$, are the grid steps in each spatial dimension. This inequality is commonly referred to as the Courant-Friedrichs-Lewy (CFL) condition and CN is the Courant number.

The EM potentials $\boldsymbol{a}$ and ϕ are related to the EM fields according to

$$\boldsymbol{e} = -\nabla\phi - \frac{\partial \boldsymbol{a}}{\partial t}, \tag{3a}$$

$$\boldsymbol{h} = \frac{1}{\mu_0}\boldsymbol{\nabla} \times \boldsymbol{a}, \tag{3b}$$

and the gauge is fixed with the Lorenz gauge, defined as

$$\boldsymbol{\nabla} \cdot \boldsymbol{a} + \frac{1}{c^2}\frac{\partial \phi}{\partial t} = 0. \tag{4}$$

In the interest of maintaining second-order accuracy, we discretize the vector potential $\boldsymbol{a}$ as a fore-vector at integer temporal steps, while the discrete scalar potential ϕ is defined at half-integer time steps. Their position on the grid is also visualized in Fig. 1. Equations (3a) and (4) are then naturally discretized as

$$\hat{\partial}_t \tilde{\boldsymbol{a}}_{\boldsymbol{m}}^{n+1} = -\tilde{\nabla}\phi_{\boldsymbol{m}}^{n+\frac{1}{2}} - \tilde{\boldsymbol{e}}_{\boldsymbol{m}}^{n+\frac{1}{2}}, \tag{5a}$$

$$\hat{\partial}_t \phi_{\boldsymbol{m}}^{n+\frac{1}{2}} = -c^2\,\hat{\nabla} \cdot \tilde{\boldsymbol{a}}_{\boldsymbol{m}}^{n}. \tag{5b}$$

Note that these equations can be interpreted as an update scheme for the EM potentials with the electric field acting as a source term.

B. Dirac Equation

The minimally coupled Dirac equation is given by

$$\imath\hbar\frac{\partial}{\partial t}\psi = \left[c\,\boldsymbol{\alpha} \cdot (-\imath\hbar\nabla - q\boldsymbol{a}) + mc^2\beta + q\phi\right]\psi, \tag{6}$$

where the complex four-component Dirac spinor

$$\psi(\boldsymbol{r}, t) = \begin{pmatrix} A(\boldsymbol{r}, t) \\ B(\boldsymbol{r}, t) \\ C(\boldsymbol{r}, t) \\ D(\boldsymbol{r}, t) \end{pmatrix}$$

is a function of position $\boldsymbol{r}$ and time t. The constants $\imath$, $\hbar$, c, m, and q denote the complex unit, the reduced Planck constant, the speed of light, the particle mass, and the particle charge, respectively. The 4×4 Dirac matrices $\boldsymbol{\alpha} = (\alpha_x, \alpha_y, \alpha_z)$ and β are defined in the traditional way.

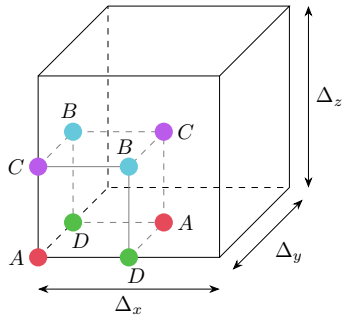

Fig. 2. The spatial grid points on which the discretized Dirac quantities are defined. The A and B components are discretized at half-integer time steps, while the C and D components are discretized at integer time steps.

1) Discretization: The discretization of the Dirac spinor is performed in accordance with [8] and is summarized as follows:

$$\begin{aligned}
A(\boldsymbol{r}, t) \quad &\text{on} \quad A_{i,j,k}^{n-\frac{1}{2}} \quad &&\text{and} \quad A_{i+\frac{1}{2},j+\frac{1}{2},k}^{n-\frac{1}{2}}, \\
B(\boldsymbol{r}, t) \quad &\text{on} \quad B_{i+\frac{1}{2},j,k+\frac{1}{2}}^{n-\frac{1}{2}} \quad &&\text{and} \quad B_{i,j+\frac{1}{2},k+\frac{1}{2}}^{n-\frac{1}{2}}, \\
C(\boldsymbol{r}, t) \quad &\text{on} \quad C_{i,j,k+\frac{1}{2}}^{n} \quad &&\text{and} \quad C_{i+\frac{1}{2},j+\frac{1}{2},k+\frac{1}{2}}^{n}, \\
D(\boldsymbol{r}, t) \quad &\text{on} \quad D_{i+\frac{1}{2},j,k}^{n} \quad &&\text{and} \quad D_{i,j+\frac{1}{2},k}^{n}.
\end{aligned}$$

A schematic representation of this stencil is shown in Fig. 2. The components of the spinor are staggered in space and time, such that the resulting discrete Dirac equation is second-order accurate in space and time. Furthermore, this staggering leads to less unknowns to solve for, a higher computational efficiency, and reduces the amount of fermion doubling [6].

This scheme was initially constructed to solve the Dirac equation by itself, but the modeling of nanoelectronic devices requires the coupling with Maxwell's equations. In [8], the Peierls substitution method is proposed to introduced the vector potential. However, this method is only an approximation and also involves computationally intensive line integrals. We propose an alternative and generally valid approach based on minimal coupling that leads to a novel update scheme for the Dirac equation influenced by an EM field. Minimal coupling introduces the extra terms $-qc\boldsymbol{\alpha} \cdot \boldsymbol{a}\psi$ and $q\phi\psi$ in (6), which we discretize as follows. First, the discrete EM potentials $\tilde{\boldsymbol{a}}$ and ϕ are interpolated to the correct grid points in space and time. Then, for the term $-qc\boldsymbol{\alpha} \cdot \boldsymbol{a}\psi$, the spinor components are interpolated along the direction corresponding to the vector component of $\boldsymbol{a}$. This method only uses central differences and interpolations, and therefore retains second-order accuracy. The result is a coupled system of eight discrete update equations, the first of which reads:

$$\begin{aligned}
\hat{\partial}_t A_{i,j,k}^{n+\frac{1}{2}} = \frac{c}{\imath\hbar}\Big[&\hat{D}_x\big|_{i,j,k}^{n} D_{i+\frac{1}{2},j,k}^{n} - \imath\hat{D}_y\big|_{i,j,k}^{n} D_{i,j+\frac{1}{2},k}^{n} \\
&+\hat{D}_z\big|_{i,j,k}^{n} C_{i,j,k+\frac{1}{2}}^{n}\Big] \\
&+ \frac{1}{\imath\hbar}(mc^2 + q\phi_{i,j,k}^{n} + V_{i,j,k}^{n})\tilde{\mathcal{M}}_t A_{i,j,k}^{n-\frac{1}{2}},
\end{aligned} \tag{7}$$

where the discrete gauge covariant derivative $\mathcal{D}$ is defined as

$$\mathcal{D}_l|^n_{i,j,k} = \partial_l - \imath q a_l|^n_{i,j,k} \mathcal{M}_l, \qquad \text{for } l = x, y, z,$$

and $\mathcal{M}_\mu$, $\mu = t, x, y, z$, is the averaging operator in each of the four space-time directions. A hat and a tilde again indicate backward and forward operators, respectively. The remaining seven update equations are determined analogously. The Dirac spinor is then updated by leveraging these eight equations in a leapfrog manner, i.e., first, A and B are advanced to time step $n + 1/2$, next, C and D to $n + 1$.

2) Stability: In this section, the dispersion relation and the stability condition of the minimally coupled Dirac scheme is derived by means of a von Neumann stability analysis. To this end, plane waves of the form

$$\psi(\boldsymbol{r}, t) = \begin{pmatrix} \mathcal{A} \\ \mathcal{B} \\ \mathcal{C} \\ \mathcal{D} \end{pmatrix} e^{\frac{\imath}{\hbar}(\boldsymbol{p}\cdot\boldsymbol{r} - Et)},$$

with constant momentum $\boldsymbol{p}$ and energy E, are placed on the stencil and inserted into the spinor update equations. The resulting 4×4 matrix system, with unknowns $\mathcal{A}$, $\mathcal{B}$, $\mathcal{C}$, and $\mathcal{D}$, only yields solutions if its determinant vanishes. Enforcing the determinant to be zero gives the discrete dispersion relation of the minimally coupled Dirac equation:

$$\begin{aligned}\left[\frac{2\hbar}{\Delta_t}\sin\left(\frac{E\Delta_t}{2\hbar}\right) - (q\phi + V)\cos\left(\frac{E\Delta_t}{2\hbar}\right)\right]^2 = \\ c^2 \sum_{l=x,y,z}\left[\frac{2\hbar}{\Delta_l}\sin\left(\frac{p_l\Delta_l}{2\hbar}\right) - q a_l \cos\left(\frac{p_l\Delta_l}{2\hbar}\right)\right]^2 \\ + \left(mc^2\right)^2 \cos^2\left(\frac{E\Delta_t}{2\hbar}\right),\end{aligned} \tag{8}$$

where we assumed for simplicity that $\boldsymbol{a}$, ϕ and V are constant in space and time. It is easily checked that in the continuum limit, i.e., $\Delta_\mu \to 0$, this equation converges to the dispersion relation of a relativistic particle in an electromagnetic field. The requirement of the energy E being real combined with the dispersion relation (8) restricts the size of the time step, which—after some tedious algebra—leads to the following stability condition:

$$\Delta_t \leq 2\hbar \sqrt{\frac{\mathcal{P}^2 + \mathcal{M}^2}{\mathcal{P}^2(\mathcal{P}^2 + \mathcal{M}^2 - \mathcal{V}^2)}}, \tag{9}$$

with

$$\begin{aligned}\mathcal{P}^2 &= c^2 \sum_{l=1}^{3}\left(\frac{4\hbar^2}{\Delta_l^2} + q^2 a_l^2\right), \\ \mathcal{M} &= mc^2, \\ \mathcal{V} &= q\phi + V.\end{aligned}$$

When the potentials are zero, it is readily verified that the stability condition (9) for the advocated minimally coupled Dirac scheme coincides with the condition found in [8], which is exactly the CFL condition (2).

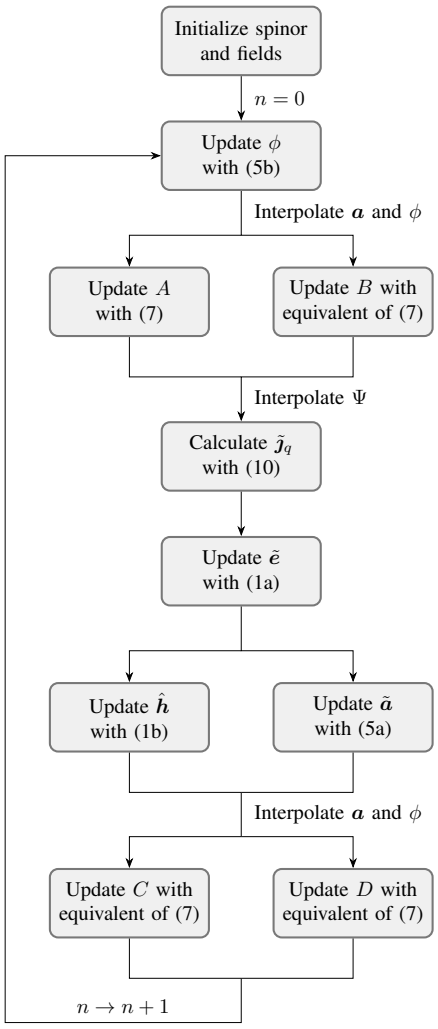

Fig. 3. Flowchart of the proposed numerical scheme for the fully coupled Maxwell-Dirac system. The line splits where the order of the updates is irrelevant. These updates can hence be computed in parallel.

C. Fully Coupled Maxwell-Dirac System

In the previous section, the forward coupling from Maxwell to Dirac was discussed. For the backward coupling, the quantum current density,

$$\boldsymbol{\jmath}_q = qc\psi^\dagger \boldsymbol{\alpha}\psi, \tag{10}$$

is introduced as an electromagnetic current source in (1a). We propose to discretize this quantity as a fore-vector at integer time steps, i.e., $\tilde{\boldsymbol{\jmath}}_q|^n_{\boldsymbol{m}}$. In order to employ (10) the spinor components are again interpolated in space and time. A self-consistent FDTD scheme of the fully coupled system is now formed by combining (1), (5), the spinor update equations (such as (7)), and (10). Fig. 3 displays the flowchart of this novel method. Note again that the incorporation of (5b) into the scheme ensures that the Lorenz gauge is exactly satisfied on the discrete level.

Due to the nonlinear nature of the coupling, a similar stability analysis of the Maxwell-Dirac scheme becomes intractable. However, through many simulation runs it was

found that if both stability conditions, (2) and (9), are satisfied, the solution remains bounded.

III. Computational Experiment: Second-Order Accuracy

In all aforementioned update equations, the continuous operators are approximated solely by second-order accurate differences and averages. Since both backward and forward coupling preserve this property, the novel fully coupled scheme is second-order accurate in space and time. This property is demonstrated by performing a range of simulations while varying the space and time steps. First, a reference simulation is run, consisting of a free particle with mass $m = 0.023 m_e$ and charge $q = -e$, where m_e and e are the electron mass and charge, respectively. The simulation space is a 3D cube with side length $6.35\,\mathrm{nm}$ that is divided into 200 cells in each direction, yielding spatial step sizes $\Delta_x = \Delta_y = \Delta_z = \Delta = 31.8\,\mathrm{pm}$. The time step is determined from (2) for a CN of 0.2, such that both stability conditions, (2) and (9), are satisfied during the entire simulation. The particle is represented as a wave packet with a Gaussian momentum profile:

$$f(\boldsymbol{p}) = e^{-\frac{p^2}{2\sigma}},$$

in which $\sigma = 2 \times 10^{-25}\,\mathrm{kg\,m\,s^{-1}}$, while all other unknowns are initially set to zero. The simulation domain is terminated with homogeneous Dirichlet boundary conditions. Note that no external sources are added, such that the appearing EM fields are generated by the particle itself. After a simulation time of $t_{\max} = 12.1\,\mathrm{as}$, the program is halted. Next, this procedure is repeated for higher values of Δ, while keeping CN and $t_{\max}$ constant. For every simulation the root-mean-square error (RMSE) with respect to the reference simulation is calculated. To this end, the reference solution is interpolated to match the grid points of the current simulation and the A and B components are interpolated in time. The resulting relations between the RMSEs and the grid step size Δ are displayed in Fig. 4. It is observed that the presented scheme for the Maxwell-Dirac equations is indeed second-order accurate in both space and time, as the error scales quadratically with the spatiotemporal step size Δ.

IV. Conclusion

In this work, we devised a novel method to solve the fully coupled Maxwell-Dirac system, targeting the accurate, multiphysics modeling of Dirac materials for integration into nanoelectronic devices. The proposed solver relies mainly on the electric and magnetic fields, rather than on the potentials, and it correctly includes the Lorenz gauge on a discrete level, unlike previous works. Minimal coupling was introduced to incorporate the influence of EM fields on the Dirac equation. By carefully discretizing the extra terms that emerged, a new solution method for the minimally coupled Dirac equation was constructed. Its stability was investigated by deriving the dispersion relation using a von Neumann stability analysis. To determine the EM fields emitted by the moving, charged

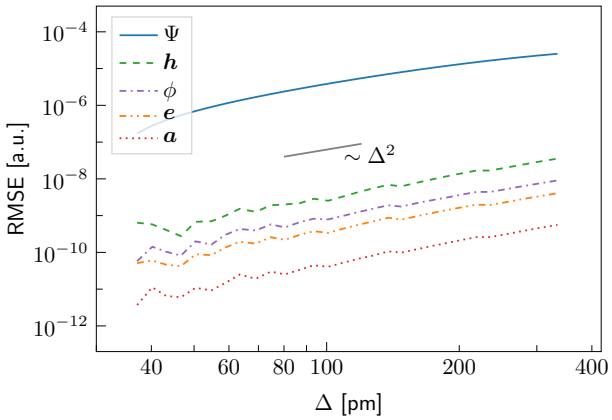

Fig. 4. The root-mean-square error (RMSE) of all pertinent quantities exhibits second-order convergence as a function of the space-time grid step Δ.

Dirac particle, the quantum current density was inserted as a current source in Ampère's law, completing the self-consistent scheme. The staggered nature of the discretization stencil grants this fully coupled method its overall second-order accuracy in both space and time, which is confirmed by a computational experiment.

Since we used the conventional finite-difference scheme for the EM fields as a starting point, the proposed method can be seamlessly integrated into existing EM-FDTD frameworks. It is possible to include, for instance, perfectly matched layers (PMLs), total-field scattered-field sources (TFSF), dielectric materials, and higher-order finite differences. These paths are open for further exploration.

References

[1] W. Bao and X. Li, "An efficient and stable numerical method for the Maxwell-Dirac system," *Journal of Computational Physics*, vol. 199, no. 2, pp. 663–687, Sep. 2004.

[2] Z. Huang, S. Jin, P. Markowich, C. Sparber, and C. Zheng, "A time-splitting spectral scheme for the Maxwell–Dirac system," *Journal of Computational Physics*, vol. 208, no. 2, pp. 761–789, Sep. 2005.

[3] X. Li, C. K. Chan, and Y. Hou, "A numerical method with particle conservation for the Maxwell-Dirac system," *Applied Mathematics and Computation*, vol. 216, no. 4, pp. 1096–1108, Apr. 2010.

[4] E. Lorin and A. Bandrauk, "A simple and accurate mixed P0-Q1 solver for the Maxwell-Dirac equations," *Nonlinear Analysis: Real World Applications*, vol. 12, no. 1, pp. 190–202, Feb. 2011.

[5] Y. Fu and L. Cao, "The Crank–Nicolson Galerkin method and convergence for the time-dependent Maxwell–Dirac system under the Lorenz gauge," *Journal of Computational and Applied Mathematics*, vol. 407, Jun. 2022, 114007.

[6] J. Smit, *Introduction to Quantum Fields on a Lattice*, ser. Cambridge Lecture Notes in Physics. Cambridge University Press, 2002.

[7] C. J. Ryu, A. Y. Liu, W. E. I. Sha, and W. C. Chew, "Finite-difference time-domain simulation of the Maxwell–Schrödinger system," *IEEE Journal on Multiscale and Multiphysics Computational Techniques*, vol. 1, pp. 40–47, Sep. 2016.

[8] R. Hammer, W. Pötz, and A. Arnold, "Single-cone real-space finite difference scheme for the time-dependent Dirac equation," *Journal of Computational Physics*, vol. 265, pp. 50–70, May 2014.

[9] W. C. Chew, "Electromagnetic theory on a lattice," *Journal of Applied Physics*, vol. 75, no. 10, pp. 4843–4850, May 1994.